scientific reports

Check for updates

OPEN

Novel L-tryptophan-functionalized zirconium dioxide nanoparticles catalysed one-pot and solvent-free synthesis of 2 H-indazolo [2, 1-b] phthalazine-triones

Ali Kareem Abbas[1], Javad Safaei-Ghomi[2]✉ & Samira Moein-Najafabadi[2]

Zirconia nanoparticles modified with L-tryptophan (ZrO_2@L-Try) demonstrate increased biocompatibility and catalytic activity by capitalizing on the bioactive properties of L-tryptophan, a crucial amino acid known for its role in protein synthesis and neurochemical functions. Successful integration of L-tryptophan onto the ZrO_2 matrix is confirmed through characterization methods. This catalytic system was employed effectively in the synthesis of 2 H-indazolo[2,1-b]phthalazine-triones through multi-component, one-pot reactions involving phthalic anhydride, various aldehydes, dimedone, and hydrazinium hydroxide under thermal, solvent-free conditions at 80 °C. Investigations suggest that ZrO_2@L-Tryptophan exhibits enhanced stability and solubility and holds promise as an innovative platform for drug delivery systems and an efficient catalyst in diverse organic reactions.

Zirconium dioxide, also referred to as ZrO_2 or zirconia, is a chemical compound consisting of zirconium and oxygen atoms[1]. This white crystalline solid has garnered significant interest across various fields due to its distinctive characteristics[2]. ZrO_2 demonstrates exceptional thermal stability, mechanical strength, and corrosion resistance, making it suitable for diverse applications[3]. With a high melting point and the ability to endure extreme temperatures, it is utilized in refractory materials, thermal barrier coatings, and crucibles for high-temperature processes[4]. Its significant oxygen ion conductivity is particularly valuable in solid oxide fuel cells (SOFCs) and oxygen sensors. In SOFCs, ZrO_2-based electrolytes facilitate the efficient conversion of chemical energy into electrical energy by aiding the transport of oxygen ions[5]. Zirconia (ZrO_2) is recognized for its exceptional biocompatibility, making it suitable for medical and dental applications. Biocompatible and wear-resistant qualities make it applicable in manufacturing dental ceramics, orthopedic implants, and artificial joints[6]. Apart from its structural applications, ZrO_2 is extensively employed as a catalyst or catalyst support in diverse chemical reactions due to its high surface area and stability, enabling it to effectively catalyze oxidation, hydrogenation, and dehydrogenation reactions[7]. Various methods, such as precipitation, sol-gel, and thermal decomposition techniques, can be used to synthesize ZrO_2, with the chosen method affecting the properties and morphology of the resulting particles[8]. In conclusion, ZrO_2 is a versatile material with diverse applications in industries such as aerospace, energy, healthcare, and catalysis, owing to its unique combination of properties that contribute to technological advancements and scientific research[9].

L-tryptophan is an essential amino acid that plays a crucial role in protein synthesis and various physiological processes in the human body[10]. It is an aromatic amino acid with a complex structure that includes a five-membered pyrrole ring and an indole group[11].

L-tryptophan, an essential amino acid, is not synthesized by the human body and must be acquired through dietary sources or supplements[12]. It is found in a variety of protein-rich foods, including meat, fish, eggs, and dairy products, as well as in specific plant-based sources such as soybeans and pumpkin seeds[13]. L-tryptophan plays a crucial role as a precursor in the biosynthesis of several important molecules, such as serotonin, melatonin, and niacin[14]. Serotonin functions as a neurotransmitter that regulates mood, appetite, and sleep[15], while melatonin serves as a hormone that controls the sleep-wake cycle[16]. Niacin, also known as vitamin B3, is vital for energy metabolism and DNA repair[17] (Fig. 1). Potential therapeutic uses of L-tryptophan have been investigated in

[1]College of Applied Medical Sciences, University of Kerbala, Kerbala, Iraq. [2]Department of Organic Chemistry, Faculty of Chemistry, University of Kashan, P.O. Box 87317-51167, Kashan, I. R. of Iran. ✉email: safaei@kashanu.ac.ir

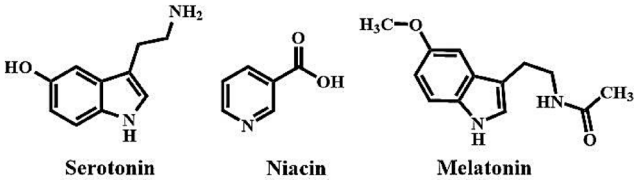

Fig. 1. Several important molecules containing the tryptophan structure.

various areas including depression, anxiety, and sleep disorders. It is believed that increasing L-tryptophan intake can elevate serotonin levels in the brain leading to improved mood and cognitive function[18]. Beyond its biological roles, L-tryptophan has found applications in various industries, such as food additives and animal feed supplements[19]. Its distinctive chemical properties have led to its utilization in the production of various organic compounds and materials[20]. In general, L-tryptophan, as an indispensable amino acid, exhibits diverse biological functions and potential therapeutic uses. Its exceptional structure and properties make it valuable across multiple scientific disciplines and industrial sectors[21].

ZrO_2@L-tryptophan is a nanocomposite material that merges the distinct characteristics of Zirconium dioxide (ZrO_2) nanoparticles with the functional properties of L-tryptophan molecules. The synthesis of ZrO_2@L-tryptophan involves attaching L-tryptophan to ZrO_2 nanoparticles to develop a composite material with enhanced properties compared to its components. ZrO_2 nanoparticles provide a large surface area, exceptional mechanical stability, and heat resistance, while L-tryptophan contributes biocompatibility and distinctive optical properties.

Overall, ZrO_2@L-tryptophan not only integrates the functional benefits of both components but also opens new avenues for research and application in therapeutic and catalytic domains. Considerable surface area and reactivity of ZrO_2 nanoparticles, combined with the functional groups of L-tryptophan, have the potential to enhance catalytic efficiency and selectivity in various chemical processes. The distinctive amalgamation of ZrO_2 and L-tryptophan within the ZrO_2@L-tryptophan nanocomposite presents promising prospects for the advancement of innovative materials and technologies across diverse domains. Additional research and investigation are necessary to comprehensively ascertain and capitalize on the potential applications of this nanocomposite.

Solvent-free organic reactions have gained significant attention due to concerns about the environmental impact of organic solvents. Synthesis of diverse and complex molecules from readily available starting materials, while considering both economic and environmental factors, is a crucial aspect of modern synthetic organic and medicinal chemistry[22]. Multi-component reactions (MCRs) that involve domino processes have emerged as powerful tools for achieving this goal. These transformations reduce the consumption of solvent, catalyst, labor, time, and energy, leading to decreased waste compared to conventional individual reactions[23,24]. Among these MCRs is the synthesis of indazolo[2,1-b]phthalazine-trione derivatives, which exhibit a wide range of biological activities[25] and show promise as fluorescence probes and luminescent materials[26].

The importance of MCRs has been recognized in various research fields including combinatorial chemistry, diversity-oriented synthesis (DOS), medicinal chemistry, and simple reaction design[27]. Furthermore, using one-pot multi-component reactions with a reclaimable core-shell catalyst can be considered a key aspect of green chemistry.

In recent years, the synthesis of nitrogen-containing heterocyclic compounds has attracted attention due to their widespread occurrence and increasing use in functional materials, agrochemicals, and biologically active pharmaceuticals[28]. Heterocyclic compounds with phthalazine moieties have garnered significant interest due to their pharmacological, biological, and clinical potential[29]. These compounds are particularly noteworthy due to their bridgehead hydrazine content and their potential for cardiotonic[30], anticancer[31], anticonvulsant[32], anti-inflammatory[33], antifungal[34], hypolipidemic[35], and vasorelaxant activities[36], as well as unique electrical and optical properties[37]. Although various catalysts have been employed for synthesizing 2 H-indazolo[2,1-b] phthalazine-triones and proven effective, some methods are limited by the need for harsh acidic conditions, transition metal catalysts, prolonged reaction times, low product yields, or additional equipment such as ultrasound[38–41]. Accordingly, developing efficient, cost-effective, and easily recoverable catalysts for this four-component reaction is essential. In line with our ongoing efforts in nanocatalyst[42] design and sustainable synthesis development, we use ZrO_2@L-tryptophan as an effective nanoparticle for the preparation of indazolo[2,1-b] phthalazine-triones through a one-pot, four-component condensation of phthalic anhydride, hydrazinium hydroxide, aromatic aldehydes, and dimedone. Reaction occurs at 80 °C under solvent-free conditions with a reusable catalyst (Fig. 2).

Experimental section

Preparation and characterization of ZrO_2@L-tryptophan as the catalyst

To synthesize ZrO_2@L-tryptophan, zirconium oxide (ZrO_2) is first prepared by dissolving zirconium salt and precipitating it with a base, calcinating the precipitate at 600–900 °C. After the ZrO_2 is obtained, L-tryptophan is dissolved in an appropriate solvent and mixed with the ZrO_2 powder, ensuring proper interaction through gentle stirring. The mixture is then dried at mild temperatures to form the composite. Characterization techniques such as XRD, FTIR, FE-SEM, TEM, TGA, EDS, and BET were employed to analyze the resulting material.

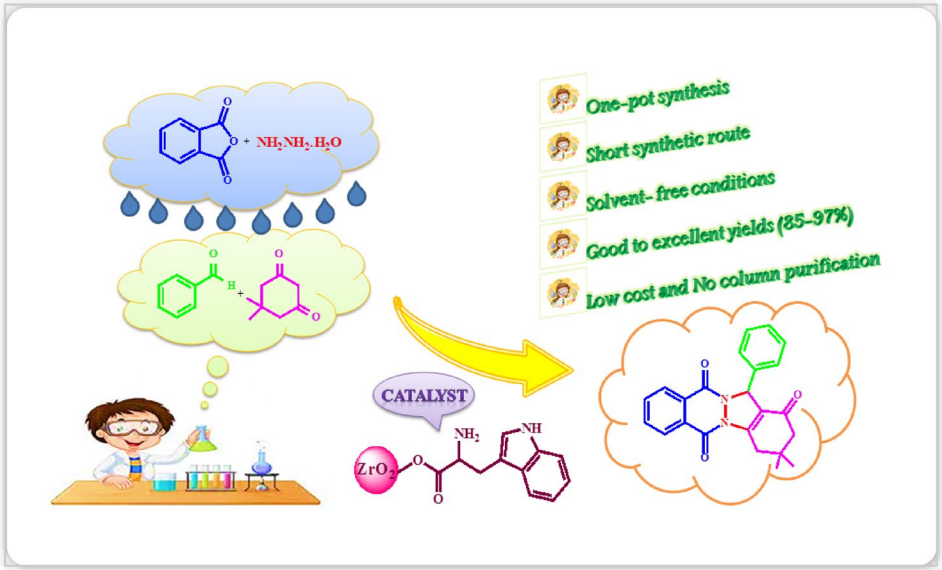

Fig. 2. One-pot four-component synthesis of 2 H-indazolo[2,1 b]phthalazine-triones catalyzed by ZrO_2@L-tryptophan.

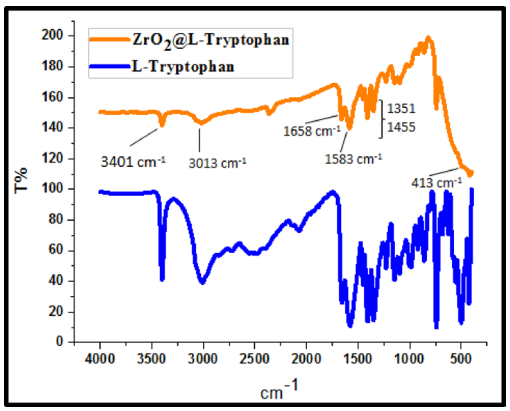

Fig. 3. Fourier transform-infrared (FT-IR) spectrum of ZrO_2@L-tryptophan.

Infrared spectroscopy (IR) analysis, shown in Fig. 3, was performed to characterize the ZrO_2@L-tryptophan composite along with its components. IR spectrum of pure L-tryptophan exhibits an absorption band around 3400 cm^{-1}, attributed to N–H and O–H stretching vibrations. This peak is also present in the ZrO_2@L-tryptophan composite, confirming the incorporation of L-tryptophan onto the ZrO_2 nanoparticles.

Additional absorption bands in the range of 1500–1600 cm^{-1} correspond to the aromatic ring vibrations of L-tryptophan, which are observable in both the pure amino acid and the composite spectra. The characteristic broad and intense absorption band around 413 cm^{-1}, assigned to the Zr–O bending vibrations, confirms the presence of zirconium oxide in the composite. Comparing the IR spectra of the individual components with the composite provides clear evidence of the successful integration of L-tryptophan with ZrO_2, as well as molecular interactions between them, without significant disruption of their characteristic functional groups.

Figure 4 displays the XRD spectra of ZrO_2, L-tryptophan, and ZrO_2@L-tryptophan. A spectrum of ZrO_2 exhibits distinct and intense peaks, indicating high crystallinity and purity. As seen in the spectrum of the final synthesized catalyst and by comparing the two previous spectra, the formation of ZrO_2@L-tryptophan is confirmed well. Analysis based on JCPDS reference cards (No. 78 – 0047 and 88-1007) reveals a mixture of monoclinic and tetragonal phases in both ZrO_2 NPs and ZrO_2@L-tryptophan structures. Peak intensity ratios indicated a predominance of the tetragonal phase, with approximately 75% of the total content[43,44]. The distinctive peaks observed in the region below 30° in the L-tryptophan spectrum are also present in the ZrO_2@L-tryptophan spectrum, confirming the successful immobilization of L-tryptophan on the nanoparticle surface without compromising the crystalline structure of the ZrO_2 core. This coexistence of peaks demonstrates the integration of both components in the nanocomposite. The average nanoparticle size of ZrO_2@L-tryptophan is calculated to be 13 nm using the Debye–Scherrer formula based on FWHM measurements from XRD

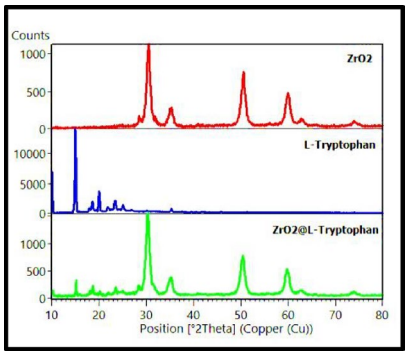

Fig. 4. X-ray diffraction patterns for ZrO_2 nanoparticles, L-tryptophan and ZrO_2@ L-tryptophan.

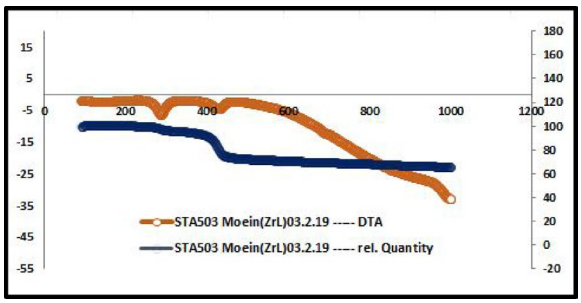

Fig. 5. The TGA and DTA curves of ZrO_2@L-tryptophan.

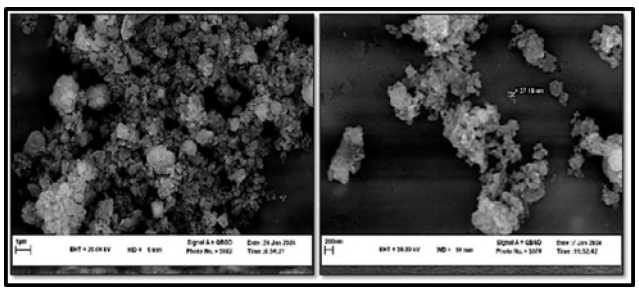

Fig. 6. The FE-SEM images of ZrO_2@L-tryptophan.

analysis, consistent with particle sizes obtained from FE-SEM and TEM analyses. The XRD results confirm the preservation of the crystalline phases of ZrO_2 nanoparticles alongside the presence of L-tryptophan, validating the successful synthesis of the ZrO_2@L-tryptophan nanocomposite.

The thermogravimetric analysis (TGA) of the ZrO_2@L-tryptophan composite was performed to assess its thermal stability and composition through weight changes as a function of temperature, as shown in Fig. 5. Thermal decomposition of the DTG process occurs during two weight-loss stages. The first stage of decomposition, below 300 °C, corresponds with the removal of decomposing terminal hydroxyl groups bonded to the surface of the zirconia. The second stage of thermal decomposition, occurring at around 400 °C and above, is attributed to the decomposition of the tryptophan group, leading to the formation of CO_2, NH_3, and H_2O molecules. The TGA curve reveals that ZrO_2@L-tryptophan NPs are stable up to 250 °C and suitable for synthesizing phthalazine compounds.

The FE-SEM analysis was used to investigate the surface morphology of the ZrO_2@L-tryptophan nanoparticles that were prepared. Figure 6 displays the FE-SEM micrographs of the ZrO_2@L-tryptophan nanoparticles at various magnifications, revealing their spherical shape and nanoscale size. The particle size measures approximately 20 nm, aligning well with the XRD data. The particles are homogeneously distributed and exhibit clear boundaries, indicating a uniform synthesis process without significant agglomeration.

Additionally, TEM analyses, depicted in Fig. 7, provided further evidence of the structural characteristics of the synthesized ZrO_2@L-tryptophan nanoparticles, showing their rounded shape and uniform distribution. High-resolution TEM images allowed for the observation of lattice fringes, confirming the crystallinity of the

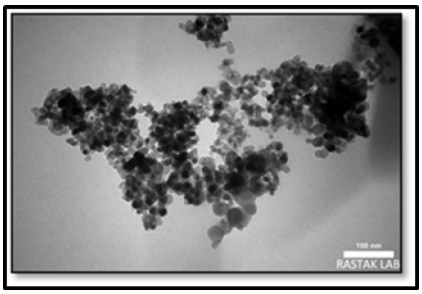

Fig. 7. Representative TEM image of the ZrO_2@L-tryptophan.

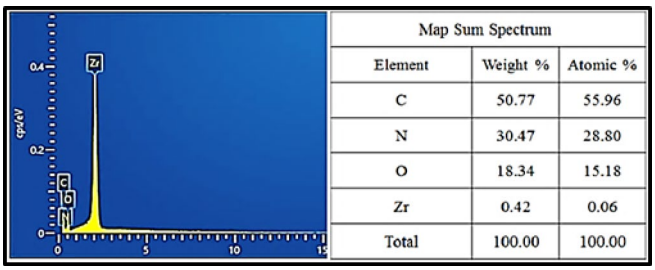

Map Sum Spectrum		
Element	Weight %	Atomic %
C	50.77	55.96
N	30.47	28.80
O	18.34	15.18
Zr	0.42	0.06
Total	100.00	100.00

Fig. 8. The EDS spectra of ZrO_2@L-tryptophan.

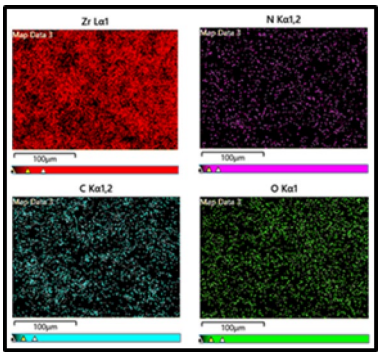

Fig. 9. Elemental mapping of ZrO_2@L-tryptophan.

nanoparticles. Selected area electron diffraction (SAED) patterns further supported the polycrystalline nature of the ZrO_2 core material. Combined analyses powerfully demonstrate that the nanoparticles possess well-defined morphology and crystal structure, corroborating the synthesis quality and consistency of the ZrO_2@L-tryptophan nanostructures.

Figure 8 presents a detailed analysis of the ZrO_2@L-tryptophan nanoparticles, demonstrating the presence of Zr, O, C, and N peaks. Formation and composition of the ZrO_2@L-tryptophan nanoparticles were confirmed through quantitative analysis, indicating high purity with no other impurities. EDS mapping was also used further to analyze the elemental state of the ZrO_2@L-tryptophan nanoparticles (Fig. 9). Despite a low percentage of Zr observed in the point-by-point EDS analysis, the distribution and dispersion in the mapping validate the effective presence of Zr and O elements.

Accurate determination of surface area and porosity is paramount for elucidating the catalytic efficacy of materials. The specific surface area and porosity of the ZrO_2@L-tryptophan catalyst were evaluated using the Brunauer-Emmett-Teller (BET) method (Figs. 10 and 11). The composite catalyst demonstrates considerable potential for a range of catalytic functions, including environmental remediation and organic transformations. BET assessment was conducted utilizing nitrogen gas as the adsorbate under liquid nitrogen conditions, generating adsorption-desorption isotherms within a relative pressure spectrum of 0.02 to 0.90. Analysis revealed a specific surface area of approximately 52.19 m^2/g, indicating a considerable available surface area for catalytic reactions, which enhances reactant adsorption and accelerates reaction rates. The total pore volume of the ZrO_2@L-tryptophan catalyst was measured to be approximately 0.2574 cm^3/g. The presence of mesoporous

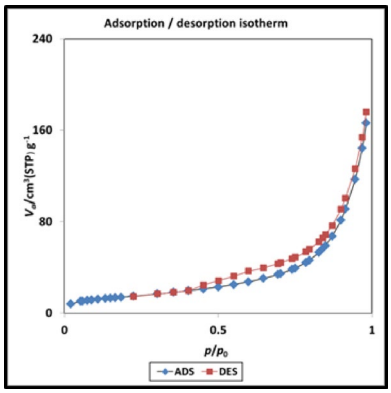

Fig. 10. N_2 adsorption/desorption isotherm curve of ZrO_2@L-tryptophan.

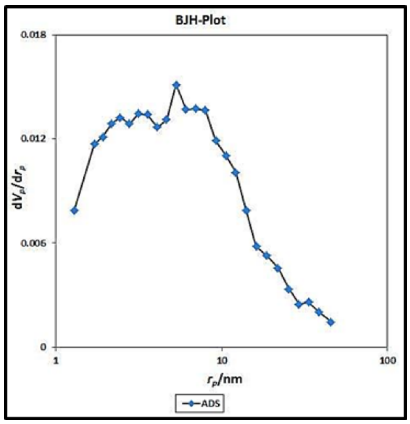

Fig. 11. Pore size distribution curve of ZrO_2@L-tryptophan.

and microporous structures promotes the effective diffusion of reactants and products throughout the catalyst matrix.

Initially, the investigation focused on the reaction involving benzaldehyde (1 mmol), dimedone (1 mmol), hydrazinium hydroxide (1.2 mmol), and phthalic anhydride (1 mmol), which served as the standard reaction. This was done using 20 mg of ZrO_2@L-tryptophan catalyst in different solvents and also without any solvent, as shown in Table 1. It was observed that the reaction progressed more efficiently under solvent-free conditions compared to reactions conducted with solvents (Table 1, entry 7). The solvent-free condition was chosen for synthesizing phthalazine derivatives. The standard reaction was conducted with varying amounts of the catalyst (Table 1, entries 9–12). The optimal result was achieved with 20 mg of catalyst. Utilizing lower amounts of ZrO2@L-tryptophan at 5, 10, and 15 mg resulted in product yields of 65%, 82%, and 88%, respectively (Table 1, entries 9–11). Increasing the amount of catalyst did not enhance the yield (Table 1, entry 12). Findings demonstrate that the catalyst significantly facilitates the transformation, as the reaction did not occur even with a longer reaction time in its absence (Table 1, entry 8). The impact of temperature was investigated by conducting the model reaction with a catalyst (20 mg) under solvent-free conditions at various temperatures (room temperature, 60, 80, and 90° C), and the most favorable outcomes were observed at 80° C (Table 1, entries 7, 13–15).

Table 2 summarizes the optimization study of different catalysts for synthesizing 2 H-indazolo[2,1-b] phthalazine-triones. ZrO_2@L-tryptophan catalyst exhibited the highest catalytic activity, affording the desired product in 96% yield within 5 min under mild reaction conditions. The individual components, ZrO_2 and L-tryptophan, showed lower efficiencies, with yields of 78% and 65%, respectively, and required longer reaction times. Tested catalysts, such as silica nanostructures, $MnFe_2O_4$ nanoparticles, and sulfuric acid, gave moderate to low yields and often involved harsher conditions or longer reactions. Results highlight the superior performance of the ZrO_2@L-tryptophan catalyst in terms of yield, reaction time, and mild conditions.

To evaluate the reactivity of ZrO_2@L-tryptophan in comparison with previously reported catalysts, a comparative summary is presented in Table 3. All catalysts listed in Table 3 achieved good yields of the desired products, several required harsh reaction conditions, including the use of toxic solvents and elevated temperatures. Some reactions demanded significantly long reaction times and specific catalysts lacked reusability. Our reusable catalyst, combined with a green methodology, offers a more efficient and environmentally friendly alternative for synthesizing the target compounds.

Entry	Catalyst amount (mg)	Solvent	Condition	Time (min)	Yield (%)[a]
1	20	H_2O	Reflux	70	45
2	20	EtOH	Reflux	40	68
3	20	EtOH-H_2O	Reflux	40	60
4	20	CH_3CN	Reflux	70	47
5	20	CH_2Cl_2	Reflux	70	52
6	20	$CHCl_3$	Reflux	70	50
7	20	Solvent-Free	80 °C	5	97
8	None	Solvent-Free	80 °C	110	-
9	5	Solvent-Free	80 °C	90	65
10	10	Solvent-Free	80 °C	15	82
11	15	Solvent-Free	80 °C	15	88
12	25	Solvent-Free	80 °C	15	90
13	20	Solvent-Free	r.t.	70	48
14	20	Solvent-Free	60 °C	10	74
15	20	Solvent-Free	90 °C	5	96

Table 1. Optimization of the amount of catalyst, solvent, and temperature in a one-pot, four component synthesis of the model reaction. Reaction conditions: benzaldehyde (1 mmol), dimedone (1 mmol), hydrazinium hydroxide (1.2 mmol), phthalic anhydride (1 mmol), ZrO_2@L-tryptophan catalyst and solvent (3 mL). [a] Isolated yield.

Entry	Catalysts	Reaction temperature (°C)	Time (min)	Yield (%)
1	Silica nanostructures	90	45	80
2	$MnFe_2O_4$ nanoparticles	90	60	75
3	Sulfuric acid (H_2SO_4)	Reflux	90	70
4	ZrO_2	90	25	78
5	L-tryptophan	90	30	65
6	ZrO_2@L-tryptophan	90	5	96

Table 2. Screening of the catalysts for the synthesis of 2 H-indazolo[2,1-b]phthalazine-triones.

Catalyst	Reaction conditions	Time (min)	Yield (%)	Ref.
p-TSA	Solvent-free/80°C	10	86	[45]
([Hnhp][HSO_4]) (5 mol%)	solvent-free, 80 °C	7	88	[46]
$Ce(SO_4)_2{\cdot}4H_2O$(10 mol%)	Solvent free, 125 °C	6	78	[47]
SBA-15 (0.02 g)	TFE, 65 °C	180	92	[48]
PEG-OSO_3H (8 mol%)	Solvent free, 80 °C	13	87	[49]
$CoFe_2O_4$-SC-SO_3H (0.5 mol%)	solvent-free, 80 °C	7	90	[50]
Fe_3O_4@SiO_2-imid-PMA[b]	Solvent-free/80°C	20	90	[39]
ZrO_2@L-tryptophan (20 mg)	Solvent free, 90 °C	5	96	This work

Table 3. Comparison of our results with previously reported methods for the synthesis of indazolophthalazinetriones.

Upon establishing the optimized parameters, we assessed the applicability of this approach by employing various aromatic aldehydes in the presence of the synthesized catalyst. Notably, a range of aromatic aldehydes, such as those with ortho-, meta-, and para-substituted aryl groups, all underwent smooth reactions under the optimized conditions, yielding the corresponding products in satisfactory to excellent yields. The results presented in Table 4 show that both electron-donating and electron-withdrawing groups efficiently yield favorable products within a short period. However, that, as expected, aldehydes containing electron-withdrawing groups, especially in the ortho and para positions, lead to the synthesis of the desired products in less time and with higher yields.

Proposed mechanism

We propose a reaction mechanism in which ZrO_2@L-tryptophan acts as a catalyst, as illustrated in Fig. 12. Mechanism consists of two steps: the initial formation of phthalhydrazide (III) through the nucleophilic addition

Entry	Aldehyde	Product	Time (min)	Yield[a] (%)	M.P.(°C)
1	C_6H_5	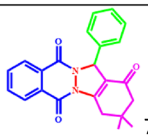 7a	5	96	205-207
2	4-OMeC_6H_4	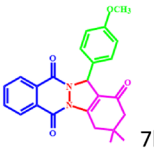 7b	10	91	216-218
3	2-Cl C_6H_4	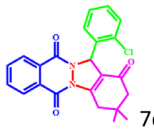 7c	4	96	267-269
4	3-ClC_6H_4	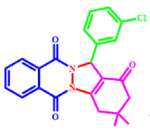 7d	5	95	203-205
5	4-ClC_6H_4	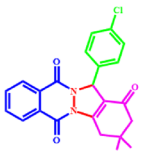 7e	4	97	261-263
6	2,4-$Cl_2C_6H_3$	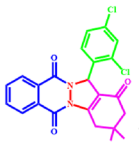 7f	4	97	221-223
7	2-$NO_2C_6H_4$	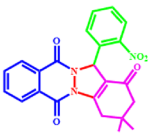 7g	4	90	235-237
8	3-$NO_2C_6H_4$	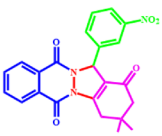 7h	6	92	274-276

Table 4. Synthesis of Indazolophthalazinetrione derivatives (7a–l) catalyzed with ZrO2@L-tryptophan at 80° C under solvent-free conditions.

of hydrazinium hydroxide (II) to phthalic anhydride (I) followed by dehydration; and the subsequent formation of heterodiene (VI) through the standard Knoevenagel condensation of dimedone (V) and aldehyde (IV). In the following step, the cooperation between this catalyst's acidic and basic functionalities facilitates the Michael-

9	4-$NO_2C_6H_4$	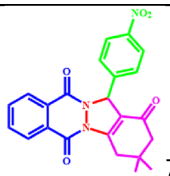 7i	5	97	220-222
10	2-MeC_6H_4	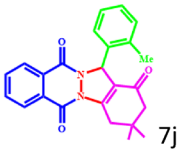 7j	10	88	230-232
11	4-MeC_6H_4	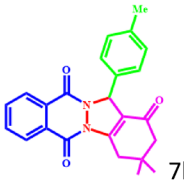 7k	10	85	227-229
12	4-BrC_6H_4	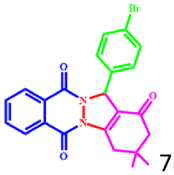 7l	7	95	266-268

Fig. 4. (continued)

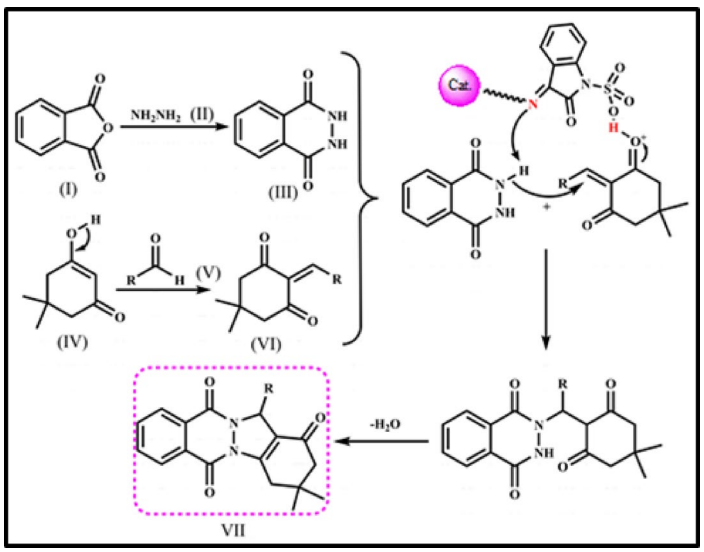

Fig. 12. Proposed mechanism for synthesis of 2 H-indazolo[2,1-b]phthalazine-triones with ZrO_2@L-tryptophan as catalyst.

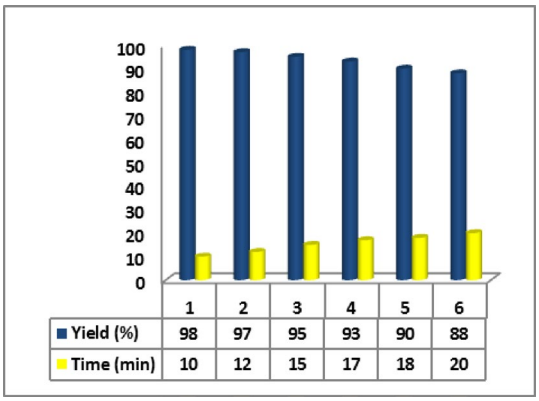

Fig. 13. Reusability of the ZrO_2@L-tryptophan nanocatalyst in the synthesis of 2 H-indazolo[2,1 b] phthalazine-triones.

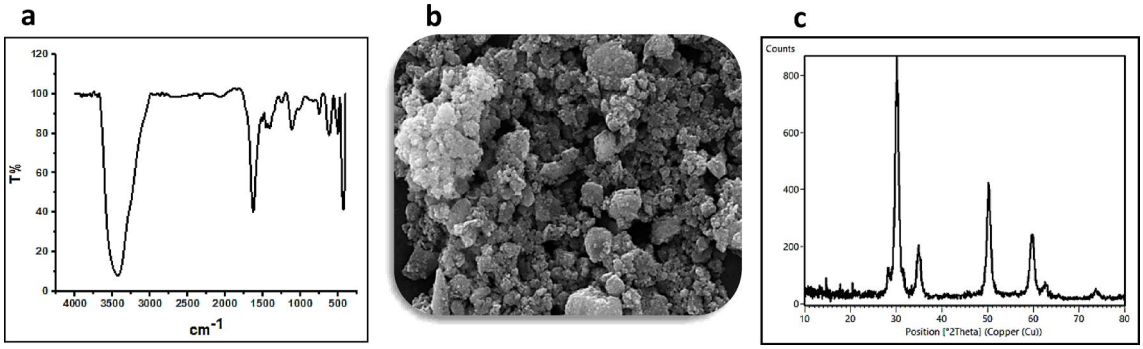

Fig. 14. FT-IR spectrum (**a**), SEM image (**b**), and XRD pattern (**c**) of the ZrO_2@L-tryptophan nanocomposite after six recycles.

Element	Experimental content (wt%)	Content after recycling (wt%)	Leaching amount (wt%)
Zr	18.3 ± 0.2	18.1 ± 0.3	< 0.01

Table 5. The Zr content in the intact ZrO2@L-tryptophan catalyst and recovered catalyst by ICP-MS.

type addition of the formed phthalhydrazide to intermediate VI. Cyclocondensation and dehydration of these intermediates result in the corresponding products (VII).

Reusability of the catalyst

The reusability of the catalyst is well-known as a key property and is essential in industrial and commercial applications, as well as in green chemistry. We have investigated the retrievability of ZrO_2@L-tryptophan NPs using the model reaction of dimedone, benzaldehyde, hydrazinium hydroxide, and phthalic anhydride. As shown in Fig. 13, the catalytic activity of ZrO_2@L-tryptophan declined from 98% in the initial run to 88% after six consecutive cycles. ZrO_2@L-tryptophan nanocatalyst was recovered by centrifugation and washed with water (10 mL) and ethyl acetate (3 × 5 mL). The obtained catalyst was dried overnight at 50 °C and reused six times without additional purification. XRD patterns, FT-IR spectrum, and SEM image (Fig. 14) of the catalyst after six runs showed that the catalyst morphology was preserved during its reuse. Moreover, ICP-OES was employed to evaluate the extent of catalyst leaching after catalytic cycles (Table 5). The concentration of zirconium in the reaction filtrates was found to be below the detection limit (less than 0.01 wt%), demonstrating excellent stability and negligible catalyst leaching under the reaction conditions. These results confirm the robustness of the ZrO_2@L-tryptophan catalyst and its suitability for multiple reuse cycles without significant loss of active sites.

General information

Chemicals

All chemicals and reagents such as $ZrOCl_2.8H_2O$, L-tryptophan, H_2SO_4, citric acid, ethylene glycol, ethanol, dimedone, hydrazinium hydroxide, phthalic anhydride, and all applied aldehydes were purchased from Merck and Fluka companies and used without any purification.

Instruments

Fourier transform infrared (FT-IR) spectroscopy was analyzed using a Nicolet Magna-400 spectrometer with KBr pellets[1]. HNMR data were gathered in DMSO-d6 using a Bruker DRX 400 spectrometer with tetramethylsilane as the internal reference. Chemical shifts are given in ppm (δ) and are referenced to the internal solvent signal. Multiplicities are declared as follows: s (singlet), bs (broad singlet), d (doublet), t (triplet), q (quartet), dd (doublet of doublets), m (multiplet). Coupling constants J are given in Hz. Powder X-ray diffraction (XRD) was performed using a Philips X'pert diffractometer with monochromatized Cu Kα radiation (λ = 1.5406 Å). The morphology of the nanoparticles was examined using field emission scanning electron microscopy (FE-SEM) with a MIRA3 model. The microscopic morphology of the nanoparticles was observed using a Philips transmission electron microscope (TEM) operating at 100 kV. The Tescan-Vega2 instrument was utilized in the academic analysis of the catalyst through electron dispersive X-rays (EDX) and mapping techniques. Thermogravimetric analysis (TGA) was performed on a Mettler TA4000 system TG-50, utilizing a heating rate of 10 K min1 in an N_2 atmosphere. The Yanagimoto micro melting point device was employed to measure the melting points without any correction.

Experimental procedures

General procedure for the synthesis of ZrO_2 nanoparticles

In 50mL of distilled water, a solution of $ZrOCl_2.8H_2O$ (0.003 mol, 0.966 g) was prepared and then mixed with citric acid (0.126 mol, 24.207 g) and ethylene glycol (0.126 mol, 7.045 mL) at room temperature. Resulting solution was stirred at 80 °C for 30 min and then refluxed for 12 h until a white sol formed. To enhance polymerization between citric acid, ethylene glycol, and $ZrOCl_2{\cdot}8\ H_2O$, the reaction mixture was cooled and then slowly heated at 80 °C for 10 h in an open bath, resulting in a more viscous wet gel. The wet gel was dried on a hot plate at 120 °C for 8 h to produce a brown powder. Brown powder was then calcined at 750 °C for 4 h at a heating rate of 4 °C/min, yielding ZrO_2 nanoparticles as a white powder.

General procedure for the synthesis of ZrO_2@L-tryptophan nanocomposites

Initially, 1 g of ZrO_2 nanoparticles was dispersed in 10 mL of dry ethanol using an ultrasonic bath for 30 min. Then, 0.5 mL of H_2SO_4 and 1.5 g of L-tryptophan were added to the solution, which was refluxed at 90 °C for 12 h. The resulting product underwent centrifugation, thorough washing with ethanol and water, and drying in a vacuum oven at 60 °C, ultimately yielding ZrO_2@L-tryptophan as a white powder.

General procedure for the preparation of 2 H-indazolo[2,1-b]phthalazine-triones in the presence of ZrO_2@L-tryptophan nanocatalyst

Aldehyde (1 mmol), 1, 3-dicarbonyl compounds (1 mmol), and ZrO_2@L-tryptophan (0.005 mol, 20 mg) were added to a mixture of hydrazinium hydroxide (1.2 mmol) and phthalic anhydride (1 mmol). The reaction mixture was heated at 80° C. After the reaction (monitored by TLC), the reaction mixture was cooled to room temperature, and ethyl acetate (5 ml) was added. Catalyst was separated by an external magnet, washed with ethyl acetate, dried, and reused under the same reaction conditions for a consecutive run. The solvent from the filtrate was evaporated under reduced pressure to obtain the crude product. Pure product was obtained by recrystallizing from a mixture of ethanol and water.

Conclusion

In our research, we have developed and characterized ZrO_2@L-tryptophan as a highly effective and reusable heterogeneous nanocatalyst. Nanoparticles were evaluated as an effective heterogeneous Lewis acid catalyst for the eco-friendly synthesis of 2 H-indazolo[1,2-b]phthalazine-triones via a one-pot, four-component condensation reaction under solvent-free conditions at 80 °C The notable advantages of this synthetic method include high efficiency, broad applicability, good to excellent product yields, short reaction times, low reaction temperature, simplicity, easy product isolation, avoidance of harmful solvents and catalysts, an environmentally friendly reaction profile, and compliance with green chemistry principles. Features make it a valuable and attractive method for synthesizing 2 H-indazolo [2, 1-b] phthalazine-triones. Catalyst is easily recovered and reused, making this method both economically and environmentally preferable for chemical industries. Catalyst can be efficiently reclaimed and used for at least six cycles without significant loss in activity.

Data availability

In terms of data availability, all the data generated or analyzed during this study can be found in the published article and its supplementary information file.

Received: 9 February 2025; Accepted: 8 July 2025
Published online: 13 July 2025

References

1. Imanova, G. T. & Kaya, M. Structural analysis of nanoparticle zirconium dioxide: a comprehensive review. *Mod. Approaches Mater. Sci.* **5**, 619–626 (2021).
2. Radu, R. D. & Drăgănescu, D. Present and future of ZrO_2 nanostructure as reservoir for drug loading and release. *Coatings* **13**, 1273 (2023).
3. Anbuchezhiyan, G., Mubarak, N. M., Ahmad, W. & Abnisa, F. Exploring the mechanical and structural properties of B_4C/ZrO_2 strengthened Al-Mg-Cr alloy hybrid composites. *J. Alloys Compd.* **980**, 173585 (2024).
4. Zhang, J. P. et al. Rapid heat treatment to improve the thermal shock resistance of ZrO_2 coating for SiC coated carbon/carbon composites. *Surf. Coat. Technol.* **285**, 24–30 (2016).
5. Fini, D., Badwal, S. P., Giddey, S., Kulkarni, A. P. & Bhattacharya, S. Evaluation of Sc_2O_3–CeO_2–ZrO_2 electrolyte-based tubular fuel cells using activated charcoal and hydrogen fuels. *Electrochim. Acta.* **259**, 143–150 (2018).
6. Singh, P. V., Reche, A., Paul, P. & Agarwal, S. Zirconia facts and perspectives for biomaterials in dental implantology. *Cureus* 15 (2023).
7. Huang, Y. & Duan, Z. Research progress on Cu-ZrO_2 catalysts: a systematic review of their preparations, doping, and applications. *J. Mater. Chem. A* (2025).
8. Yang, C. et al. Modified wet chemical method synthesis of nano-ZrO_2 and its application in Preparing membranes. *Ceram. Int.* **47**, 13432–13439 (2021).
9. Raj, R. & Singh, G. A review on process prerequisites and biomedical applications of additively manufactured zirconia. *Eng. Sci. Technol. Int. J.* **59**, 101876 (2024).
10. Richard, D. M. et al. L-tryptophan: basic metabolic functions, behavioral research and therapeutic indications. *Int. J. Tryptophan Res.* **2**, IJTR–S2129 (2009).
11. Shimazaki, Y., Yajima, T. & Yamauchi, O. Properties of the Indole ring in metal complexes. A comparison with the phenol ring. *J. Inorg. Biochem.* **148**, 105–115 (2015).
12. Lopez, M. J. & Mohiuddin, S. S. Biochemistry, essential amino acids. In *StatPearls*. StatPearls Publishing (2024).
13. Singh, R. B. Role of Tryptophan in health and disease: systematic review of the anti-oxidant, anti-inflammation, and nutritional aspects of Tryptophan and its metabolites. *World Heart J.* **11**, 161–178 (2019).
14. Sutanto, C. N., Loh, W. W. & Kim, J. E. The impact of Tryptophan supplementation on sleep quality: a systematic review, meta-analysis, and meta-regression. *Nutr. Rev.* **80**, 306–316 (2022).
15. Vaseghi, S., Arjmandi-Rad, S., Nasehi, M. & Zarrindast, M. R. Cannabinoids and sleep-wake cycle: the potential role of serotonin. *Behav. Brain. Res.* **412**, 113440 (2021).
16. Bueno, A. P. R., Savi, F. M., Alves, I. A. & Bandeira, V. A. C. Regulatory aspects and evidences of melatonin use for sleep disorders and insomnia: an integrative review. *Arq. Neuropsiquiatr.* **79**, 732–742 (2021).
17. Gasperi, V., Sibilano, M., Savini, I. & Catani, M. V. Niacin in the central nervous system: an update of biological aspects and clinical applications. *Int. J. Mol. Sci.* **20**, 974 (2019).
18. Jenkins, T. A., Nguyen, J. C., Polglaze, K. E. & Bertrand, P. P. Influence of Tryptophan and serotonin on mood and cognition with a possible role of the gut-brain axis. *Nutrients* **8**, 56 (2016).
19. Ren, X. et al. A comprehensive review and comparison of L-tryptophan biosynthesis in Saccharomyces cerevisia e and Escherichia coli. *Front. Bioeng. Biotechnol.* **11**, 1261832 (2023).
20. Darabi, H. R. et al. A novel approach to l-tryptophan grafting on mesoporous MCM-41: A recoverable heterogeneous material for organocatalyzed benzo [N, N]-heterocyclic condensation. *J. Mol. Struct.* **1311**, 138453 (2024).
21. Hou, Y., Li, J. & Ying, S. Tryptophan metabolism and gut microbiota: a novel regulatory axis integrating the microbiome, immunity, and cancer. *Metabolites* **13**, 1166 (2023).
22. Kohansal, M. Advances in green chemistry: sustainable approaches in organic synthesis. *Int. J. New. Chem.* **12**, 726–737 (2025).
23. Moein-Najafabadi, S. & Safaei-Ghomi, J. Silica/APTPOSS anchored on $MnFe_2O_4$ as an efficient nanomagnetic composite for the Preparation of spiro-pyrano [2, 3-c] Chromene derivatives. *BMC Chem.* **18**, 155 (2024).
24. Veisi, H., Manesh, A. A., Khankhani, N. & Ghorbani-Vaghei, R. Protic ionic liquid [TMG][Ac] as an efficient, homogeneous and recyclable catalyst for one-pot four-component synthesis of 2 H-indazolo [2, 1-b] phthalazine-triones and dihydro-1 H-pyrano [2, 3-c] pyrazol-6-ones. *RSC Adv.* **4**, 25057–25062 (2014).
25. Salehi, P. & MaGee, D. I. Minoo dabiri, Laleh Torkian & Jordan Donahue. *Mol. Divers.* **16**, 231–240 (2012).
26. Mazaahir, K., Ritika, C. & Anwar, J. Efficient CAN catalyzed synthesis of 1 H-indazolo [1, 2-b] phthalazine-1, 6, 11-triones: an eco-friendly protocol. *Chin. Sci. Bull.* **57**, 2273–2279 (2012).
27. Mohlala, R. L., Rashamuse, T. J. & Coyanis, E. M. Highlighting multicomponent reactions as an efficient and facile alternative route in the chemical synthesis of organic-based molecules: a tremendous growth in the past 5 years. *Front. Chem.* **12**, 1469677 (2024).
28. Yu, H. & Xu, F. Advances in the synthesis of nitrogen-containing heterocyclic compounds by in situ benzyne cycloaddition. *RSC Adv.* **13**, 8238–8253 (2023).
29. Mourad, A. K., Makhlouf, A. A., Soliman, A. Y. & Mohamed, S. A. Phthalazines and phthalazine hybrids as antimicrobial agents: synthesis and biological evaluation. *J. Chem. Res.* **44**, 31–41 (2020).
30. NOMOTO, Y. et al. Studies on cardiotonic agents. II.: synthesis of novel phthalazine and 1, 2, 3-benzotriazine derivatives. *Chem. Pharm. Bull.* **38**, 2179–2183 (1990).
31. Fedorov, O. et al. [1, 2, 4] Triazolo [4, 3-a] phthalazines: inhibitors of diverse bromodomains. *J. Med. Chem.* **57**, 462–476 (2014).
32. Sun, X. Y., Wei, C. X., Deng, X. Q., Sun, Z. G. & Quan, Z. S. Synthesis and primary anticonvulsant activity evaluation of 6-alkyoxyl-tetrazolo [5, 1-a] phthalazine derivatives. *Arzneimittelforschung* **60**, 289–292 (2010).
33. Liu, D. C., Gong, G. H., Wei, C. X., Jin, X. J. & Quan, Z. S. Synthesis and anti-inflammatory activity evaluation of a novel series of 6-phenoxy-[1, 2, 4] Triazolo [3, 4-a] phthalazine-3-carboxamide derivatives. *Bioorg. Med. Chem. Lett.* **26**, 1576–1579 (2016).
34. Ryu, C. K., Park, R. E., Ma, M. Y. & Nho, J. H. Synthesis and antifungal activity of 6-arylamino-phthalazine-5, 8-diones and 6, 7-bis (arylthio)-phthalazine-5, 8-diones. *Bioorg. Med. Chem. Lett.* **17**, 2577–2580 (2007).
35. Masihpour, F., Zare, A., Merajoddin, M. & Hasaninejad, A. Highly effectual protocol for the production of Triazolo [1, 2-a] indazole-triones and 2-indazolo [2, 1-b] phthalazine-triones using 1, 3-disulfonic acid imidazolium hydrogen sulfate as a dual-functional catalyst. *J. Chem. Technol. Metall.* **54**, 23–29 (2019).
36. Watanabe, N. et al. 4-Benzylamino-1-chloro-6-substituted phthalazines: synthesis and inhibitory activity toward phosphodiesterase 5. *J. Med. Chem.* **41**, 3367–3372 (1998).
37. Litvinov, V. P. Multicomponent cascade heterocyclisation as a promising route to targeted synthesis of polyfunctional pyridines. *Rus. Chem. Rev.* **72**, 69–85 (2003).
38. Amirmahani, N., Mahmoodi, N. O., Malakootian, M. & Pardakhty, A. Introducing new and effective catalysts for the synthesis of Pyridazino [1, 2-a] indazole, Indazolo [2, 1-b] phthalazine and Pyrazolo [1, 2-b] phthalazine derivatives. *MethodsX* **7**, 100823 (2020).
39. Esmaeilpour, M., Javidi, J., Dodeji, F. N. & Zahmatkesh, S. Solvent-free, sonochemical, one-pot, four-component synthesis of 2 H-indazolo [2, 1-b] phthalazine-triones and 1 H-pyrazolo [1, 2-b] phthalazine-diones catalyzed by Fe_3O_4@ SiO_2-imid-PMA n magnetic nanoparticles. *Res. Chem. Intermed.* **47**, 2629–2652 (2021).
40. Habibi, D. & Shamsian, A. An efficient and recyclable bifunctional acid–base ionic liquid for synthesis of 1 H-indazolo [1, 2-b] phthalazinetriones. *Res. Chem. Intermed.* **41**, 6245–6255 (2015).

41. Afzalian, B., Mague, J. T., Mohamadi, M., Ebrahimipour, S. Y. & Kermani, E. T. Ni (II), Co (II), and Cu (II) complexes incorporating 2-pyrazinecarboxylic acid: synthesis, characterization, electrochemical evaluation, and catalytic activity for the synthesis of 2H-indazolo [2, 1-b] phthalazine-triones. *Chin. J. Catal.* **36**, 1101–1108 (2015).
42. Moein Najafabadi, S. & Safaei Ghomi, J. Synthesis of COF-SO_3H immobilized on manganese ferrite nanoparticles as an efficient nanocomposite in the Preparation of spirooxindoles. *Sci. Rep.* **13**, 22731 (2023).
43. Muthuselvi, C., Arunkumar, A. & Rajaperumal, G. Growth and characterization of oxalic acid doped with Tryptophan crystal for antimicrobial activity. *Der. Chem. Sin.* **7**, 55–62 (2016).
44. Reddy, C. V., Babu, B., Reddy, I. N. & Shim, J. Synthesis and characterization of pure tetragonal ZrO2 nanoparticles with enhanced photocatalytic activity. *Ceram. Int.* **6**, 6940–6948 (2018).
45. Sayyafi, M., Seyyedhamzeh, M., Khavasi, H. R. & Bazgir, A. One-pot, three-component route to 2H-indazolo [2, 1-b] phthalazine-triones. *Tetrahedron* **64** (10), 2375–2378 (2008).
46. Shaterian, H. R. & Aghakhanizadeh, M. Four-component synthesis of 2H-indazolo [2, 1-b] phthalazine-1, 6, 11 (13H)-trione derivatives. *Comp. Rendus Chim.* **15** (11–12), 1060–1064 (2012).
47. Mosaddegh, E. & Hassankhani, A. A rapid, one-pot, four-component route to 2H-indazolo [2, 1-b] phthalazine-triones. *Tetrahedron Lett.* **52** (4), 488–490 (2011).
48. Rostamnia, S. & Doustkhah, E. A mesoporous silica/fluorinated alcohol adduct: an efficient metal-free, three-component synthesis of Indazolophthalazinetrione heterocycles using a reusable nanoporous/trifluoroethanol adduct (SBA-15/TFE). *Tetrahedron Lett.* **55** (15), 2508–2512 (2014).
49. Hasaninejed, A., Kazerooni, M. R. & Zare, A. Solvent-free, one-pot, four-component synthesis of 2H-indazolo [2, 1-b] phthalazine-triones using sulfuric acid-modified PEG-6000 as a green recyclable and biodegradable polymeric catalyst. *Catal. Today.* **196** (1), 148–155 (2012).
50. Zhao, X. N. et al. A highly efficient and recyclable Cobalt ferrite Chitosan sulfonic acid magnetic nanoparticle for one-pot, four-component synthesis of 2 H-indazolo [2, 1-b] phthalazine-triones. *RSC Adv.* **4** (93), 51089–51097 (2014).

Acknowledgements

The authors gratefully acknowledge the University of Kashan for providing facilities for this work.

Author contributions

A.K.A. Designed and Conducted some of the experiments and wrote the manuscript. S. M-N. discussed the experiments, analyzed the results, and rewrite the manuscript. J. S-G. supervised the whole project.

Declarations

Competing interests

The authors declare no competing interests.

Additional information

Supplementary Information The online version contains supplementary material available at https://doi.org/10.1038/s41598-025-11227-z.

Correspondence and requests for materials should be addressed to J.S.-G.